2001-05

A Neural Circuit for Coordinating Reaching with Grasping: Autocompensating Variable Initial Apertures, Perturbations to Target Size, and Perturbations to Target Orientation

A neural circuit for coordinating reaching with grasping: Autocompensating variable initial apertures, perturbations to target size, and perturbations to target orientation

Antonio Ulloa and Daniel Bullock

May, 2001

Technical Report CAS/CNS-01-007

Boston University Center for Adaptive Systems and
Department of Cognitive and Neural Systems
677 Beacon Street
Boston, MA 02215

A Neural Circuit for Coordinating Reaching with Grasping: Autocompensating Variable Initial Apertures, Perturbations to Target size, and Perturbations to Target Orientation

Antonio Ulloa*& Daniel Bullock†
Boston University
Deparment of Cognitive and Neural Systems
677 Beacon St, Boston MA 02215 USA
aup@bu.edu, danb@cns.bu.edu

May 29, 2001

Abstract

A neural network model is presented, that extends principles of the VITE (vector integration to end-point) model [1, 2, 3, 4] of primate reaching to the more complex case of reach-grasp coordination. The main new planning problem addressed by the model is how to simulate human data on temporal coordination between reaching and grasping, while at the same time remaining stable and compensating for altered initial apertures and perturbations of object size and object location/orientation. Simulations of the model replicate key features of four different experimental protocols with a single set of parameters. The proposed circuit computes reaching to grasp trajectories in real-time, by continuously updating vector positioning commands, and with no precomputation of total or component movement times. The model consists of three generator channels: transport, which generates a reaching trajectory; aperture, which controls distance between thumb and index finger; and orientation, which controls hand orientation vis-a-vis target's orientation.

1 Introduction

The act of reaching and grasping is usually divided into two distinct components: hand transport and hand aperture control. The transport component consists of a single phase which involves the movement of the wrist from an initial position to a final position that

*Supported by CONACYT of México
†Supported by DARPA/ONR N00014-95-1-0409

is close to the object to be reached. The aperture component consists of two sequential phases: preshape, which opens the hand to a maximum aperture, and enclosing, which reduces the aperture until the fingers contact the object. A third component, wrist orientation, quantifies the change in wrist orientation with respect to the arm, so that the hand is in a feasible position to grasp the object.

The features of a prehension movement can be appreciated by describing the transport kinematics and aperture formation. The transport velocity exhibits a unimodal, symmetrical velocity profile typical of point-to-point movements. The hand aperture shows an opening to a maximum aperture, and then closing to the object size. Furthermore, there is a parallel evolution of both processes, such that they initiate and terminate approximately simultaneously. The question arises as to how the timing of the two processes is coordinated in a way that is robust, that is, that naturally adapts to perturbations. The present paper addresses this question, to show how a biologically-based neural network can model adaptive coordination in reaching to grasp static objects.

1.1 Data constraints

There is a temporal landmark for occurrence of maximum hand aperture (MA) with respect to movement time (MT). Wallace and Weeks [5] instructed subjects to grasp a small object at different distances and within a specified MT. MA was observed to occur at 61-67.8% of MT. Similarly, Jeannerod [6], using different object widths and distances, found a small band of relative timing of MA (74%-81%). Further, Paulignan and Jeannerod [7] reported MA occurrence at 70-80% of MT, and Jakobson and Goodale [8] noted MA to occur right after 2/3 of MT.

Larger MAs have been empirically associated with faster movements. Wing et al [9] instructed subjects to grasp objects at two speeds, normal and fast. The normal speed was chosen by the subject and the fast one was as fast as possible without dropping the object. It was observed that when movements were faster, MA was larger.

Experiments with an initially wide hand aperture show a tight coupling between reach and grasp, especially at the end of movement. Saling et al [10] experimented with two types of grasping, normal and altered. A normal grasp initiated with the fingers relaxed, whereas an altered grasp initiated with the fingers maximally extended. Representative trials of those experiments are shown in the left column of Fig. 2, which depicts, for the altered case, an initial aperture reduction phase followed, sometimes after a pause (zero value of the velocity trace), by a small or no reopening of the grip aperture, and then the final enclosing phase. In addition, the enclosing phase appeared to begin at or just before the time typical for normal prehension.

Switching to a new target object causes a reduction in aperture and then a reopening, as well as an elongation of MT. Paulignan et al. [11] investigated the effects of perturbations to object location on the coordination between transport and aperture control. In these experiments, the position of the object was unexpectedly shifted at movement onset. Two transparent objects were used, and the illumination could be switched from one object to the other. The objects were located at either 20^o and 10^o or 20^o and 30^o with respect to the body midline. Both components, transport and aperture, were affected by the perturbation. MT was elongated to allow for corrections in movement. Paulignan et al reported a

250-290 ms delay before correction of the wrist trajectory and a lengthening by 100 ms of MT.

When object size is perturbed, MT is lenghtened, as needed for corrections. Paulignan et al. [12] conducted experiments with small and large objects. The objects were transparent, and either the small or the large one was illuminated. The perturbations of object size were introduced at movement onset. The left column of Fig. 3 illustrates the effects of small-to-large (S-L) and large-to-small (L-S) perturbations on the grasping kinematics. In the S-L perturbation, the grip aperture first increases to the peak corresponding to the small object, and then increases again to a maximum aperture corresponding to the large object, to finally close around the object. The S-L perturbation gave rise to an elongation of MT.

1.2 Prior models of reach-grasp coordination

1.2.1 The Hoff-Arbib model

In the Hoff and Arbib model [13], estimated times for transport and opening are applied to coordinate transport with aperture control. First, prior to movement initiation, reaching distance and object size are estimated, based on visual information. Next, reaching distance and object size are used to estimate transport MT, and object size is used to estimate opening time (OT). Then, enclose time (ET), which is assumed constant for a particular task, is added to OT, to form a second estimated MT. Finally, the maximum of the two MT estimates is used as the actual transport MT. To compute OT, ET is then subtracted from MT. Thus the model adjusts the component times to accomodate the fixed ET.

After the pre-movement stage, transport and opening controllers are activated concurrently; opening controller goal achievement triggers the activation of an enclose controller. The transport controller is a feedback controller with a cost function that penalizes inaccuracy, variability, and lack of smoothness in the movement trajectory. The controllers for opening and enclose are feedback controllers with an optimization criterion that assigns costs to hand opening and closing acceleration. We sought a model that could explain the data without such pre-timing and optimization computations.

1.2.2 The Haggard-Wing model

In the Haggard and Wing [14] model, both processes, transport and aperture control, have access to each other's spatial state. The model performs on-line error-driven corrections of a trajectory from a present position, P_i, to a target position, T_i. Coupling terms made each component dependent on the other's activity:

$$\begin{bmatrix} \Delta P_T \\ \Delta P_A \end{bmatrix} = \begin{bmatrix} \alpha & \beta \\ \gamma & \delta \end{bmatrix} \begin{bmatrix} DV_T \\ DV_A \end{bmatrix},$$

where DV_T is the difference between transport target position (T_T) and the current hand position (P_T); and DV_A is the current difference between target aperture (T_A) and present aperture (P_A). ΔP_T and ΔP_A are increments in position that drive the states of transport

and aperture towards their target states. Coupling constants α and δ are the influence that each component's DV exerts over its own position change, whereas β is the influence that DV_A exerts over P_T, and γ is the influence that DV_T exerts over P_A. With these fixed gains, the algorithm is executed iteratively, continuously updating DV_T and DV_A. The effect of reaching a MA larger than object size is achieved by the influence of the constant gain γ of the transport component's effect over the aperture component. To improve the realism of the velocity profiles produced by this spatial generator, an extension made T_i move from the initial P_i values to their final values at a constant velocity [see 15]. We sought a model that avoided an unbiological "constant velocity" assumption.

2 Methods

2.1 Circuit structure

The planning problem in reaching and grasping coordination is how to ensure that the aperture and orientation rates are scaled to ensure completion in approximately the same time allowed by the transport phase. The coordination of these processes must be robust to allow natural adaptations when perturbations occur. We here introduce a neural network model, based on the VITE model of trajectory generation [1, 2, 3, 4] that reproduces key features of reaching and grasping coordination. The proposals of this model are: (1) arm transport, hand aperture, and wrist orientation are parallel yet interdependent processes. Coupling from both transport and orientation to aperture quantify the influence that transport and orientation velocities exert on the magnitude of hand aperture. Therefore, larger maximum apertures associated with faster movements are generated as a consequence of those influences; (2) arm transport, hand aperture, and wrist orientation are gated by a common internal GO signal, which enables synchronous completion of reaching and grasping. No precomputation of component movement times is necessary; (3) discrepancies between current perceived and internal representation of positions are detected by cells that transiently inhibit the volitional GO signal, thereby avoiding jerky motions and preserving temporal equifinality despite unexpected changes in target location, target size, or target orientation; (4) hand aperture evolves continually under the influence of a self-inhibition, due to passive biomechanical effects, that causes a tendency of the hand to close. This influence is especially manifested when there is no voluntary control acting on the hand, and is stronger for larger apertures.

2.2 Heuristics

The proposed circuit, illustrated in Fig. 1, works as follows. Subscripts T, A, and O stand for transport, aperture, and orientation. The differences between targets, T_i, and the inputs for perceived targets, I_i, are integrated by T_i cells. Differences between present positions, P_i, and T_i are registered in D_i. Movement is initiated when the GO signal becomes active, triggering activation of velocity cells, V_i. V_is are integrated by their respective P_i, but there is also influence from V_T and V_O over P_A. Note that P_A, unlike P_T and P_O, is influenced by strong self-inhibition (through inhibitory neuron R). This influence captures

the hypothesis that the hand always tends to return to a semiclosed or relaxed position, even when there is no volitional movement. E_i Cells represent discrepancies between perceived targets and internal representations of targets. If, after movement is initiated, any of the targets is modified, E_i cells will inhibit the GO signal, thereby slowing movement execution and allowing time for corrections. Also, when there is no target in any of the I_is, the corresponding T_i will remain equal to P_i, thereby allowing independent execution of any module.

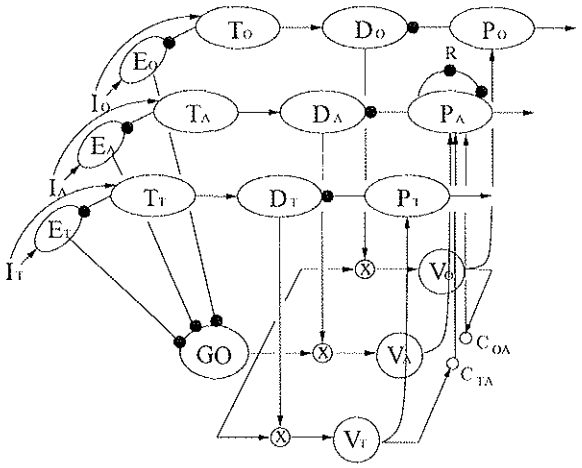

Figure 1: Reach-grasp coordination circuit. Links terminated by filled balls are inhibitory.

Transport component. The transport component obeys

$$\dot{D_T} = \alpha(-D_T + T_T - P_T), \tag{1}$$

$$\dot{V_T} = \alpha_V(-V_T + g_0 G_2 [D_T]^+), \tag{2}$$

$$\dot{P_T} = V_T, \text{ and} \tag{3}$$

$$\dot{T_T} = \alpha(-T_T + I_T), \tag{4}$$

where g_0 and G_2 are the gating amplitude and GO signal, respectively. Parameters α and α_V were set to 30 and 300, respectively.

Aperture component. The aperture component obeys

$$\dot{D_A} = \alpha(-D_A + T_A - P_A), \tag{5}$$

$$\dot{V_A} = \alpha_V(-V_A + g_0 G_2 D_A), \tag{6}$$

$$\dot{P_A} = V_A + C_{TA} + C_{OA} - \beta R, \text{ and} \tag{7}$$

$$\dot{T_A} = \alpha(-T_A + I_A), \tag{8}$$

where C_{TA} is the influence that transport velocity exerts on aperture and C_{OA} is the influence that orientation velocity exerts on aperture. Note that P_A undergoes self-inhibition through R, where $\dot{R} = \alpha(-R + P_A)$. The parameter associated with this self-inhibition, β, was set to 3.5. It is important to observe in Eq. 6 that D_A is not half-wave rectified. This

is a convenient simplification. Neural signals are typically half-wave rectified, and the present simplification could be replaced by a push-pull arrangement of two oppositely polarized half-wave rectified D_A processes, as implemented in some other versions of VITE.

Orientation component. This component obeys

$$\dot{D_O} = \alpha(-D_O + T_O - P_O), \tag{9}$$

$$\dot{V_O} = \alpha_V(-V_O + g_0 G_2[D_O]^+), \tag{10}$$

$$\dot{P_O} = V_O, \text{ and} \tag{11}$$

$$\dot{T_O} = \alpha(-T_O + I_O). \tag{12}$$

Note that the orientation component was introduced to account for studies on target orientation perturbation [11]. If target orientation remains unaltered in a grasping task, the orientation component stays inactive and, therefore, has no effect on aperture formation.

GO signal. The GO signal is the output, G_2, of a cascade of two shunting cells,

$$\dot{G_1} = -G_1 + (B - G_1)k_1 - G_1(\gamma E_T + \delta E_A + \epsilon E_O), \tag{13}$$

$$\dot{G_2} = -G_2 + (B - G_2)G_1 - G_2(\gamma E_T + \delta E_A + \epsilon E_O), \tag{14}$$

where $B = 20$, $k_1 = 0.01$, $\gamma = 5$, $\delta = 15$ and $\epsilon = 10$. Signals E_T, E_A, and E_A are outputs of cells that register the discrepancies, if any, between current target parameter values and perceived targets. When location, orientation, or size targets are altered during reach to grasp execution, E_i signals allow such alterations to inhibit the GO signal momentarily, thereby slowing down the movement in proportion to current GO value and allowing time for corrections. Thus, movement time is lengthened whenever such disturbances occur. It is important to mention that there are two types of coupling: direct coupling, which is implemented by explicit state coupling terms in the aperture equations; and indirect parameter coupling, which is mediated via effects on the GO signal.

Discrepancies between perceived and internal targets.

$$\dot{E_i} = \alpha(-E_i + abs(I_i - T_i)), \tag{15}$$

where $i = \{T, A, O\}$.

Coupling neurons.

$$\dot{C_{jA}} = \alpha(-C_{jA} + \rho_j V_T), \tag{16}$$

where $j = i \neq A$, and $\rho_T = \rho_O = 0.5$. The coupling from V_T and V_O to P_A causes a maximum aperture that exceeds object size and scales with transport velocity and orientation change velocity.

3 Results

Basic features of prehension. The model reproduced the basic features of a normal prehension movement. Transport velocity exhibited a bell shaped velocity profile typical of point-to-point arm movements [1, 16]. The plot of hand aperture showed the hand opening to its maximum aperture, then decreasing until it reached object size.

Zero vs. Large initial apertures. Saling et al's experiments [10] with normal (closed) or large initial apertures were simulated, and the model dynamics are depicted on the right-hand side of Fig. 2.

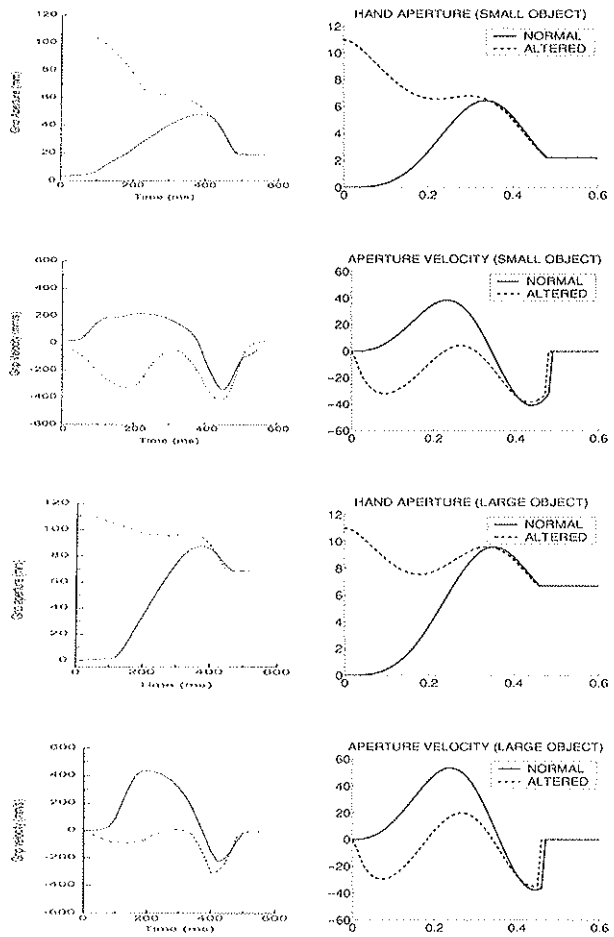

Figure 2: Zero vs. large initial apertures. Data plots are on the left (reproduced from [10]) and simulations on the right. Object sizes were 2.2 and 6.7 cm. Object location was 30 cm. Altered initial aperture was 11 cm. GO amplitude was set to 60.

Perturbations to object orientation. Simulations of object switching [11] were done. Paulignan et al [11] reported lengthening of MT by 100 ms on average. When the perturbation was registered by the model at $t = 180$ ms, to reflect a visual processing delay, such a lengthening also occurred in the model.

Perturbations to object size. Simulation results of grasping when object size was unexpectedly perturbed [12] are illustrated in right column of Fig. 3. Aperture and aperture velocity are shown, for perturbed as well as for normal grasping. The perturbation was registered by the model at $t = 200$ ms (not 180 ms), based on data [17] indicating slower visual processing in the object size than in the object location streams.

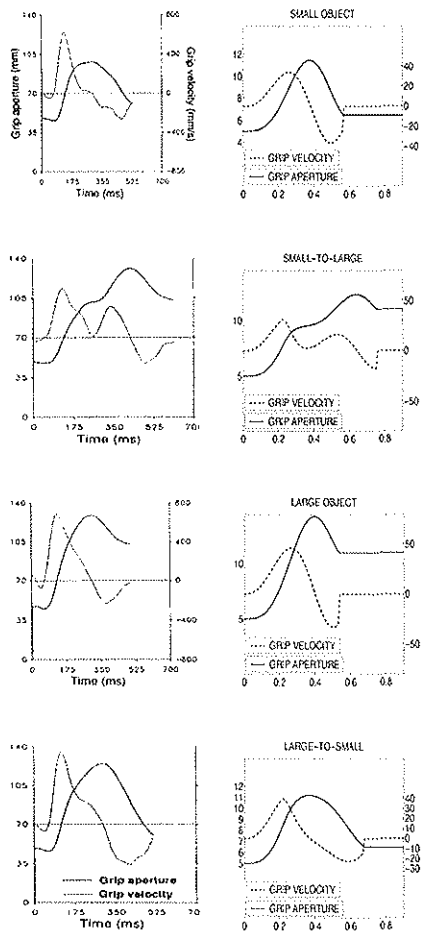

Figure 3: Perturbations to target size. Data plots are on the left (reproduced from [12]) and simulations on the right. Object sizes were 1.5 and 6 cm. Object location was 35 cm. GO amplitude was set to 40.

For a full range of GO amplitudes, the model shows consistent relative timing of maximum apertures. Figure 4 portrays the timing of reaching to grasp components over various simulations using a full range of GO amplitudes. Increments of the GO amplitude increases the speed at which the grasp is made. The relative timing of occurrence of maximum aperture (70.6–75%) is maintained over the range of speeds.

For a full range of object sizes, the model shows consistent relative timing of maximum apertures, as well as an emergent trend. Fig. 5 depicts the timing of the components of grasping when simulations were run over a full range of experimental object sizes. As in the previous figure, the relative timing of maximum aperture shows consistency with values found

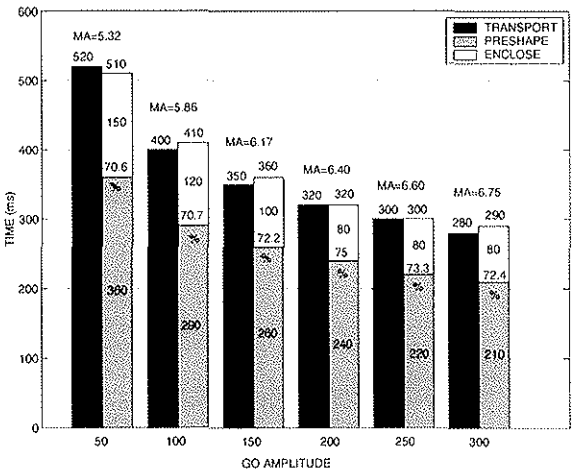

Figure 4: Durations (msec) of transport, grasp, preshape and enclose for a range of GO amplitudes. Numbers on top of bars are transport and grasp durations. Numbers inside bars are preshape and enclose durations. Percentages reflect relative timing of MA with respect to transport time. Transport distance and object size were 24 and 2.2 cm, respectively.

in the literature (63.8–84%). With regard to enclose time, there exists an emergent trend showing the enclose time decreasing as the object size increases. This is in accord with an empirical observation of Hofsten and Rönnqvist [18] The reason behind this trend in the model is that although the maximum aperture increases linearly with object size, the slope (at 0.65) is less than one, so the aperture overshoot is signficantly less for a large than for a small object. Thus the distance to be travelled in the final closure is actually less for grasping large objects than small objects. Castiello et al [19] also observed that when grasping objects of different sizes, the maximum aperture occured later for a larger object. Since occurence of maximum aperture marks the beginning of the enclose time, it is possible to consider Castiello et al's observation as implicating that enclosing times are longer for smaller objects, which confirms the above studies and the simulations.

Also, Figs. 4 and 5 show other data-consistent properties of the model, such as larger MAs for faster movements [9] and larger MAs for larger targets.

4 Discussion

Successful prehension across a wide range of contexts requires adaptive coordination between the different mechanical degrees of freedom that contribute to the act. Across acts of prehension, objects of grasp change in their positions relative to the body, their orientations relative to the body, their sizes, their shapes, and their mechanical properties, such as surface friction, compressibility and mass distribution. In this paper, we have focused on three aspects of the kinematic control and coordination problems – transport, orientation, and aperture – that respectively arise from object variations in position, orientation, and size. It was argued that VITE-type trajectory generators based on gated integration

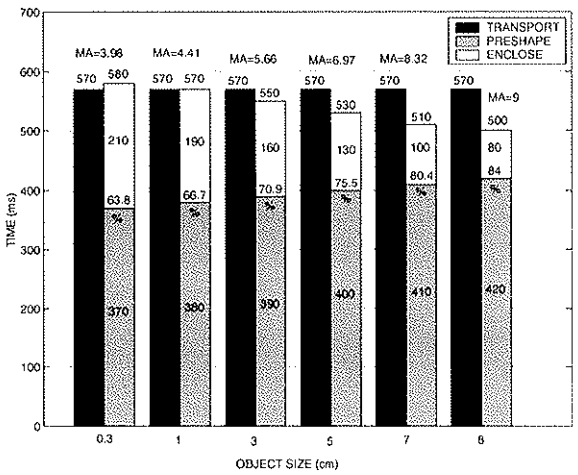

Figure 5: Durations (msec) of transport, grasp, preshape and enclose for a range of object sizes. Numbers on top of bars are transport and grasp durations. Numbers inside bars are preshape and enclose durations. Percentages reflect relative timing of MA with respect to transport time. Transport distance was set to 24 cm. GO amplitude was set to 40.

of difference vectors computed between desired and current states could provide the fundamental competence needed to adapt to the three types of object variations addressed. Any three controllers acting on a single system like the hand-arm are of necessity coupled by mechanical interactions if they are sensitive to evolving feedback signals. However, in this study, we ignored such interactions in order to focus on the question of what internal couplings, within the command system itself, could serve as a basis for robust responses to object variations. In principle, multiple controllers acting in parallel could be spatially coupled, temporally coupled, or both. Moreover, such coupling could occur only at selected times, or continuously. In the Hoff and Arbib model, there was no spatial coupling, and the temporal coupling occurred only prior to movement onset. In the Haggard and Wing model, there was continuous spatial coupling but no temporal coupling. The model proposed here employs continuous temporal and spatio-temporal (velocity) coupling, and in that sense adopts ideas from both prior models. However, using the VITE generator as a basis allowed a solution that eliminated any need for pre-computation of component times (as in the Hoff and Arbib) or for a two-stage construction of realistic velocity profiles (as in the Haggard and Wing model). In particular, temporal coupling was achieved by using a common GO signal to control the onset, perturbation-induced slowing, and normative speeding of the vector integration process in all three controllers. Provided that this GO signal grows during the prehension movement, it provides a robust basis for temporal equifinality [2] of the controller cycles, and thus for synchronous termination of transport, hand reorientation, and aperture closure to grasp the object. A notable property is that this design easily and automatically compensates for variability in sensory processing delays. For example, it can autocompensate if, as reported empirically, the pathway computing object location is faster than that computing object size.

Regarding spatial coupling, a surprising finding of our simulations was that there was no need, as in the Hoff and Arbib model, to sequentially program separate "maximum"

and "final" apertures for the hand. Instead, it sufficed to allow the transport and orientation velocity control signals to have a proportionate effect on the hand aperture. Spatial cross-coupling via these signals naturally causes a transient hand aperture overshoot that is larger in movements with faster transport or faster re-orientations. Both compensations serve the purpose of helping to avoid contact of the hand with the object before the fingers are ready to close upon it. The speed-accuracy tradeoff that characterizes all movements implies that fast transport or reorientation movements will be less accurate. This reduced accuracy raises the risk of hand collision with the object "on the way in", a risk that can be avoided by increasing aperture.

Because arm position and wrist orientation affect the hand significantly, but not vice-versa, there was no reason to introduce reciprocal links from aperture velocity to the other two controllers. Thus the model connectivity is not symmetrical. Another aspect of broken symmetry in the model is the assumption of a spontaneous relaxation of the aperture to a closed resting position. Although implemented nominally as a central process, our thesis is that it reflects a passive biomechanical factor. Such passive closure seems more natural than active closure as an explanation of the transient early overshoot of aperture reduction in the "altered" trials of [10].

These simple provisions for temporal and spatio-temporal coupling allowed the model to recreate all the cited empirical trends regarding aperture size variations and relative timing of maximum aperture vis-a-vis the transport MT. Moreover, the model was able to provide a good appoximation of the qualitative dynamics exhibited by the full range of movements treated.

References

[1] D. Bullock and S. Grossberg. Neural dynamics of planned arm movements: Emergent invariants and speed-accuracy properties during trajectory formation. *Psychological Review*, 95(1):49–90, 1988.

[2] D. Bullock and S. Grossberg. The VITE model: A neural command circuit for generating arm and articulator trajectories. In J.A.S. Kelso, A.J. Mandell, and M.F. Shlesinger, editors, *Dynamic Patterns in Complex Systems*, pages 305–326. World Scientific, Singapore, 1988.

[3] D. Bullock, P. Cisek, and S. Grossberg. Cortical networks for control of voluntary arm movements under variable force conditions. *Cerebral Cortex*, 8(1):1–15, January 1998.

[4] D. Bullock, R.M. Bongers, M. Lankhorst, and P.J. Beek. A vector-integration-to-endpoint model for performance of viapoint movements. *Neural Networks*, 12:1–29, 1999.

[5] S.A. Wallace and D.L. Weeks. Temporal constraints in the control of prehensile movement. *Journal of Motor Behavior*, 20(2):81–105, 1988.

[6] M. Jeannerod. The timing of natural prehension movements. *Journal of Motor Behavior*, 16(3):235–245, 1984.

[7] Y. Paulignan and M. Jeannerod. Prehension movements. the visuomotor channels hypothesis revisited. In A.M. Wing, P. Haggard, and J.R. Flanagan, editors, *Hand and Brain: The Neuro-*

physiology and Psychology of Hand Movements, chapter 13, pages 265–282. Academic Press, London, 1996.

[8] L.S. Jakobson and M.A. Goodale. Factors affecting higher-order movement planning: A kinematic analysis of human prehension. *Experimental Brain Research*, 86:199–208, 1991.

[9] A.M. Wing, A. Turton, and C. Fraser. Grasp size and accuracy of approach in reaching. *Journal of Motor Behavior*, 18(3):245–260, 1986.

[10] M. Saling, S. Mescheriakov, E. Molokanova, G.E. Stelmach, and M. Berger. Grip reorganization during wrist transport: the influence of an altered aperture. *Experimental Brain Research*, 108:493–500, 1996.

[11] Y. Paulignan, C. MacKenzie, R.G. Marteniuk, and M. Jeannerod. Selective perturbation of visual input during prehension movements. 1. The effects of changing object position. *Experimental Brain Research*, 83:502–512, 1991.

[12] Y. Paulignan, M. Jeannerod, C. MacKenzie, and R. Marteniuk. Selective perturbation of visual input during prehension movements. 2. The effects of changing object size. *Experimental Brain Research*, 87:407–420, 1991.

[13] B. Hoff and M.A. Arbib. Models of trajectory formation and temporal interaction of reach and grasp. *Journal of Motor Behavior*, 25(3):175–192, September 1993.

[14] P. Haggard and A. Wing. Coordinated responses following mechanical perturbation of the arm during prehension. *Experimental Brain Research*, 102:483–494, 1995.

[15] A.G. Feldman. Once more on the equilibrium-point hypothesis (lambda model) for motor control. *Journal of Motor Behavior*, 18:17–54, 1986.

[16] H. Nagasaki. Asymmetric velocity and acceleration profiles of human arm movements. *Experimental Brain Research*, 74:319–326, 1989.

[17] J. Tannee, D. Boussaoud, N. Boyer-Zeller, and E.M. Rouiller. Direct visual pathways for reaching movements in the macaque monkey. *NeuroReport*, 7(1):267–272, 1995.

[18] C. von Hofsten and L. Rönnqvist. Preparation for grasping an object: A developmental study. *Journal of Experimental Psychology: Human Perception and Performance*, 14(4):610–621, 1988.

[19] U. Castiello, G.E. Stelmach, and A.N. Lieberman. Temporal dissociation of the prehension pattern in Parkinson's Disease. *Neuropsychologia*, 31(4):395–402, 1993.